Journal of Engineering Research and Applied Science
Available at www.journaleras.com
Volume 12 (2), December 2023, pp 2322-2336
ISSN 2147-3471 © 2023

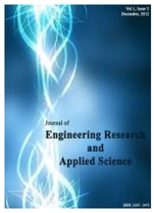

Petrography, Mineral Chemistry and Crystallization Conditions of Oligocene Aged Alabalık Volcanics (Oltu-Erzurum, NE Turkey)

Emre Aydınçakır

Gumushane University, Geological Engineering, Gumushane, Türkiye

Accepted 10 August 2023

Abstract
In this study, mineralogical, petrographic, and mineral chemistry analyses of Oligocene-aged Alabalık volcanic rocks (Oltu/Erzurum) in the Eastern Pontides (NE, Türkiye) were revealed. The studied volcanic rocks consist of andesitic, dacitic, and pyroclastic. These rocks consist of plagioclase (An_{15-44}), hornblende (Mg# = 0,632-0,80), biotite (Mg# = 0,62-0,657), augite ($Wo_{44}En_{42}Fs_{15}$), and Fe-Ti oxide minerals. They generally exhibit hyalomicrolytic porphyritic, glomera porphyritic, cumulative porphyritic, microlitic porphyritic, poikilitic and intersertal textures. In the studied rocks, disequilibrium textures are observed such as oscillatory zoning, sieve texture and corrosion in plagioclase phenocrysts, and resorbed cores and mantles, rounded crytals, and embayed rims in clinopyroxenes. According to thermobarometric calculations, the crystallization temperatures, pressures and oxygen fugacity values of the studied volcanic rocks range from 800 ºC to 1027 ºC, 0.7 to 8.8 kbar, and -15.2 to -9.0, respectively. The amphibole-derived estimated water content in the studied volcanic rocks vary from 2.6 to 8.2%. Al these features suggests that the magmas that forms the studied volcanic rocks had undergone hydrous crystallizations in the shallow to mid-crustal magma chambers.

Keywords: *Mineral chemistry, geothermobarometer, Alabalık volcanic, Oltu, NE Turkey*

1. Introduction
The Eastern Pontide orogenic belt is located east of the Sakarya Zone in the Northern Turkey (Figure 1) and can be considered as one of the most complex and significant segments of the Alpine-Himalayan system due to successive subduction-collision events. The Eastern Pontides are considered a well-preserved arc system (Figure 1), formed of the northward subduction of the Neo-Tethyan oceanic crust beneath the Eurasian plate. Many authors have studied the geodynamic evolution of the region [1-11].

The post-collision geodynamics of the Sakarya Zone in Northeastern Turkey is still actively debated. Recent studies suggest that post-collision extensional tectonics may have started in the Early Eocene period [2, 9, 12-14]. Post-collision magmatism in the eastern Sakarya Zone occurred in an extensional setting beginning from the Early Eocene and persisted over a 15-million-year time interval [7, 15-16], for approximately 10 million years. Subsequently, due to compressional forces from the Oligocene to the Miocene, the eastern part of the Sakarya Zone was uplifted above sea level [6, 9]. In the Miocene, the Sakarya Zone and the Eastern Anatolian plateau were uplifted [3, 17]. The aim of this study is to investigate the detailed petrography and mineral chemistry of the volcanic rocks observed in the Alabalık region (Oltu-Erzurum). Based on the analyses results, the crystallization conditions of the magmas that formed the volcanic rocks are interpreted in conjunction with regional geology. The study intends to explore the processes of magma development within the crust that led to the formation of these rocks.

2. Regional geology and stratigraphy
The oldest units in the Eastern Pontide Orogenic Belt consist of metamorphic basement rocks from the Early to Middle Carboniferous period, including gneiss, schist, amphibolite, marble, and minor metaperidotites. [18-21] (Figure 1). These rocks are occupied by Middle Carboniferous - Early Permian plutonic rocks [21-27]. Late Carboniferous shallow marine-continental sedimentary rocks, which lie unconformably on metamorphic ground rocks, are observed only in the Pulur region [28-29]. Jurassic

[a]Corresponding author: aydincakir61@gmail.com

rocks in the Eastern Pontides include sedimentary rocks containing pyroclastic and clastic [30]. The pre-Jurassic basement rocks are cut by Early and Middle Jurassic intrusive rocks [31-34]. In the Late Cretaceous, the Eastern Pontide magmatic arc developed with northward subduction of the Neo-Tethys along the Sakarya Zone [2-3]. Adakitic and non-adakitic rocks with Early Eocene age (54-48 My) occurred in the final stage of arc-continent collision [12-13, 35-36]. During the Middle Eocene, post-collisional volcano-sedimentary rocks and calc-alkaline shoshonitic plutons developed [6, 8-11, 37-41]. Miocene-Pliocene-Quaternary volcanic rocks, mostly alkali with lower rates of calc-alkali composition, are the youngest representatives of magmatic activity in the Eastern Pontides [8, 14, 39, 42-46].

The basis units in the study area located in the Alabalık (Oltu, Erzurum) region is the Eocene aged Narman Volcanics, consisting of basalt, andesite and pyroclastics. This unit is unconformably overlain by the Oltu Formation, which consists of yellow-red-green colored conglomerate, sandstone and mudstone, containing Oligo-Miocene aged white colored gypsum and limestone interlayers and coal seams. Alabalık Volcanic rocks [49], consisting of Oligocene aged lavas and agglomerates, conformably overlie the Oltu Formation (Figure 2). Quaternary alluviums are the youngest unit.

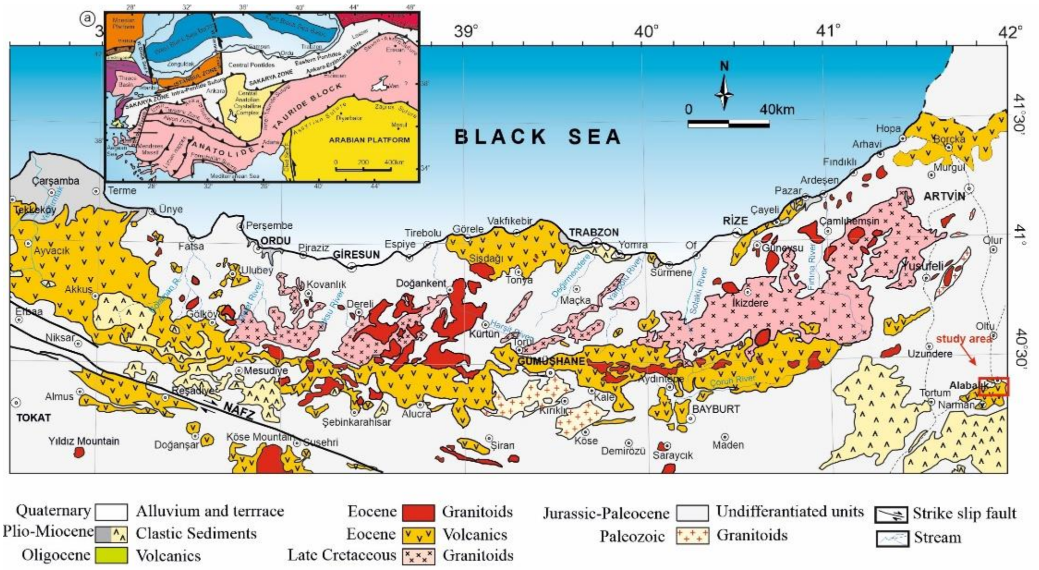

Figure 1. (a) The tectonic units and the main suture zones of Turkey after [47]; (b) the simplified geological map of the Eastern Pontides showing distribution of the Eocene and Oligocene-Miocene–Quaternary volcanic rocks (Modified after [48], [7], and [11]).

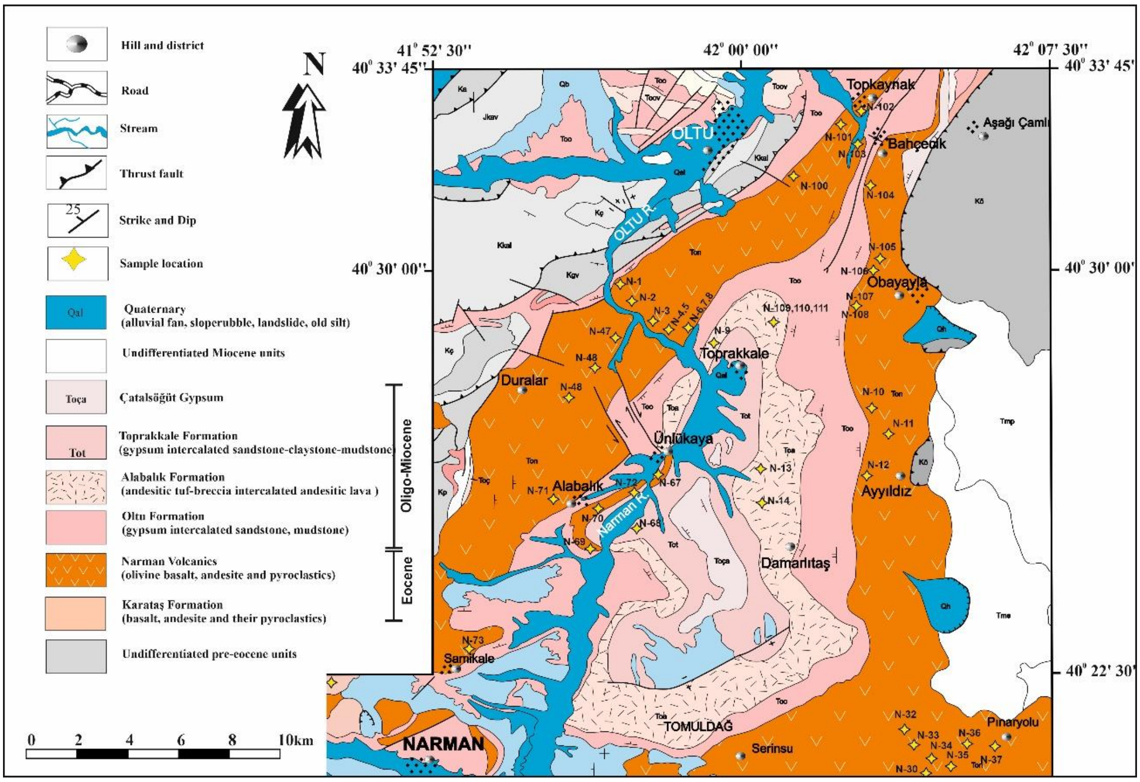

Figure 2. (a) The geological map of the Alabalık (Oltu-Erzurum) area, and the sample locations.

3. Material and Method

During field studies, the rock samples were collected using a GPS device from the volcanic rocks and the surrounding rocks associated with these rocks. Significant surfaces were photographed and documented. Based on the data obtained from all these field studies, a 1/25.000 scale geological map of the region [48] was prepared (Figure 2). Thin sections were prepared to determine the mineralogical and petrographic characteristics of the volcanic rock samples taken from the study area. Plates of 0.5x2x4 cm dimensions were taken from the rocks, and after removing the roughness of one surface, they were attached to a 2.5x5 cm glass with Canada balsam, with a thickness of 1 mm. The rock attached to the glass was thinned with abrasives up to a thickness of 0.025 mm to prepare it for petrographic examination. Thin section samples were prepared in the Thin Section Laboratory of the Faculty of Engineering and Natural Sciences, Gümüşhane University, Department of Geological Engineering.

Mineral chemistry analyses were performed at Bretagne Occidentale University Geoscience Marines (IFREMER) Electron Microprobe Laboratory located in Brest (France). Samples for mineral chemistry analysis with a CAMECA-SX-100 WDS brand device were prepared as carbon-coated polished sections. The device setting was 15 kV electron bombardment and 20 nA bombardment flow. The count time for Si, Al, Ti, Fe, Mn, Mg, Ca, Na and K elements was set to 10 s. Analyses of hornblende and Fe-Ti oxides used 1 µm point ray while feldspar and mica mineral analyses used slightly defocused (10 µm) rays to prevent losses due to sodium evaporation. Analyses used natural mineral standards of forsterite, diopside, orthoclase, albite, anorthite, biotite, apatite, wollastonite and magnetite. Analyses were carried out with analytic error less than 1% for major elements and less than 200 ppm for trace elements.

4. Results

4.1. Petrography

This unit consisting mainly of yellow-green tuff and agglomerates was originally distinguished as "Alabalık Tuff" by [49]. However, due to its inclusion of various lithologies such as lavas, agglomerates, epiclastics, and others, its name was later changed to the "Alabalık Formation."

The unit is represented by yellow-green-colored, generally thick-bedded or massive tuffs and agglomerates. Agglomerates occur as thick and poorly stratified layers (Figure 3a, b). Intercalations of light-colored andesites are also present. Microscopic examination of the andesites reveals a porphyritic texture, containing plagioclase (andesine), hornblende, and minor pyroxene phenocrysts; the groundmass is devitrified volcanic glass (Figure 3).

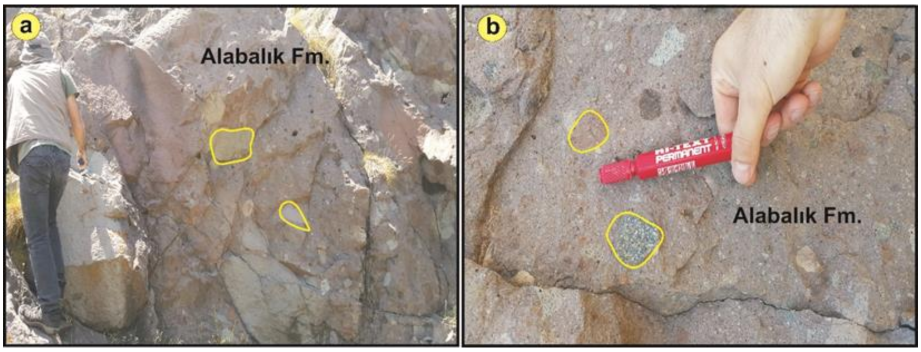

Figure 3. (a, b) Appearance of various-sized andesitic breccia fragments constituting the Alabalık Formation.

Alabalık volcanic rocks shows generally hyalo-microlitic porphyritic, fluidal, and occasionally cumulophyric textures. Petrographically, the rocks are composed of plagioclase (plj), hornblende (hbl), biotite (bi), clinopyroxene (cpx), and opaque minerals (op). Plagioclases are generally observed as large euhedral-shaped phenocrysts or megacrystals. A spongy texture is observed at the edges of the plagioclase and outermost resorption rims and generally exhibits slight zoning. The sieve textures and resorption rims observed in these minerals can indicate disequilibrium crystallization and magma mixing [50]; Figures 4a-d).

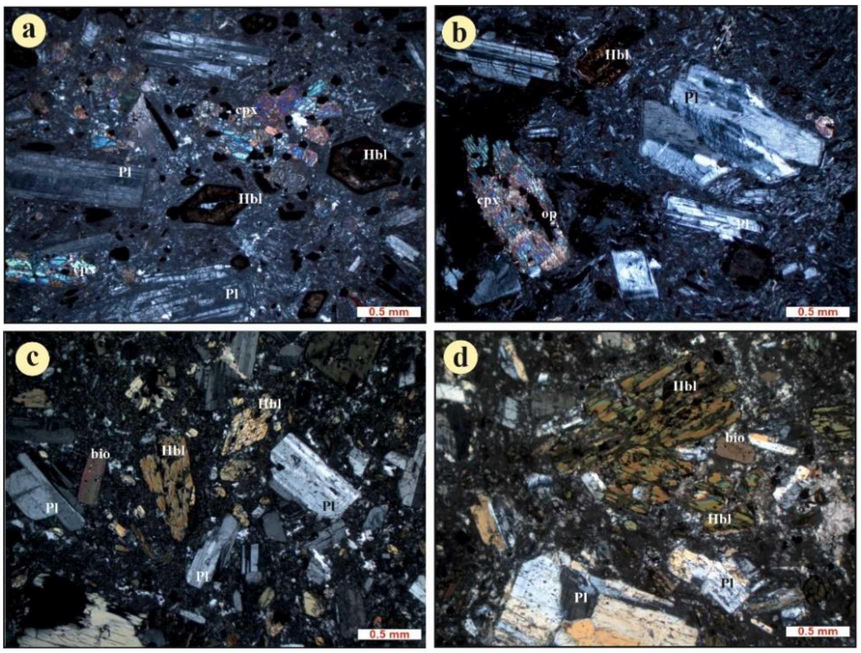

Figure 4. photomicrography showing of andesites within the Alabalık volcanic rocks. (a) Plagioclase phenocryst showing albite twinning and sieve texture, cumulophyric texture exhibited by clinopyroxenes, and euhedral opaque hornblende minerals, (b) Clinopyroxene phenocryst containing opaque mineral inclusions and opacification from the edges, (c) Euhedral hornblende and biotite minerals, (d) Hornblende minerals exhibiting glomeroporphyritic texture (Cpx: Clinopyroxene, Pl: Plagioclase, Hbl: Hornblende, Bio: Biotite, Op: Opaque mineral).

Some hornblende crystals also exhibit corrosion and resorption. Biotites are generally observed as euhedral phenocrysts, but sometimes they are also seen as subhedral or anhedral relic crystals (Figures 4c and d). They exhibit a pleochroism in colors ranging from light brown to dark brown. There are occasional opacifications and chloritization on the edges. Clinopyroxenes generally occur as euhedral and subhedral grains. They often show twinning, and some crystals have resorption rims on their edges (Figures 4a and b). Fe-Ti oxides are generally observed as inclusions in hornblende and clinopyroxene minerals in small irregular shapes and sometimes as angular grains in the groundmass (Figures 4a-d). Both phenocrystic and microlitic hornblendes, generally, have euhedral to subhedral crystals (Figure 4), and opacification is observed in the margins (Figure 4c-d).

4.2. Mineral Chemistry

4.2.1. Plagioclase

Plagioclases occur as subhedral to euhedral phenocrystals and microlites. They display commonly normal and reverse-zoned. They are seen as phenocrysts and microlites within other minerals in the form of inclusions. Plagioclases also commonly exhibit albite twinning and sieve textures.

Plagioclase, which is mostly observed as phenocryst in andesites, is generally in the composition of oligoclase and andesine (An_{44-15}) (Table 1, Figure 5). The phenocryst plagioclase comprises compositions ranging from An_{44} to An_{15} in the core, and from An_{48} to An_{31} in the rim, respectively. The composition of the microlites is andesine, ranging between An_{45} and An_{37}. In samples showing reverse zoning, the core compositions range between An_{15} and An_{42}, while the rim compositions vary between An_{34} and An_{48} (Figure 5).

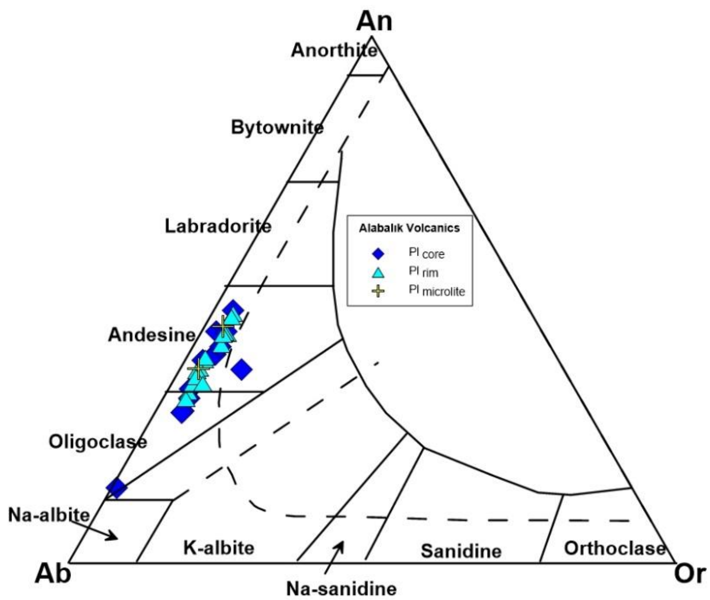

Figure 5. The Ab-An-Or diagram for plagioclase in andesites within the Alabalık volcanic rocks.

4.2.2. Hornblende

One of the important ferromagnesian minerals observed in the Alabalık volcanic rocks in the Oltu (Erzurum) region is hornblende. Hornblendes are generally twinned, large, and euhedral to subhedral, often found in association with biotite and Fe-Ti oxide minerals (Figures 6a and b). Their edges are partially opaque, and they exhibit well-developed twinning in two directions (Figures 6a and b). According to [50], the opacifications occurring along the cleavages and edges of hornblendes are explained by the release of volatiles in the crystal during the rise of the magma to shallower sections and the reaction of the crystal with the melt. According to [51], the samples are classified as calcic compositions (Figure 7a) and are magnesio-hastingsite, pargasite, and edenite (Figure 7b). The Mg# (Mg number) of amphiboles varies from 0.63 to 0.80.

[a]Corresponding author: aydincakir61@gmail.com

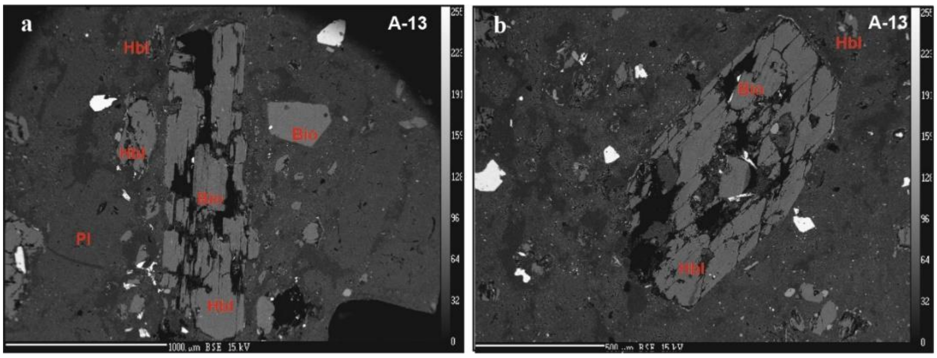

Figure 6. The 'BSE' (Backscattered Electron) images of the hornblendes, a, b) Some of large hornblendes contain biotite (Bio) and opaque minerals (Op).

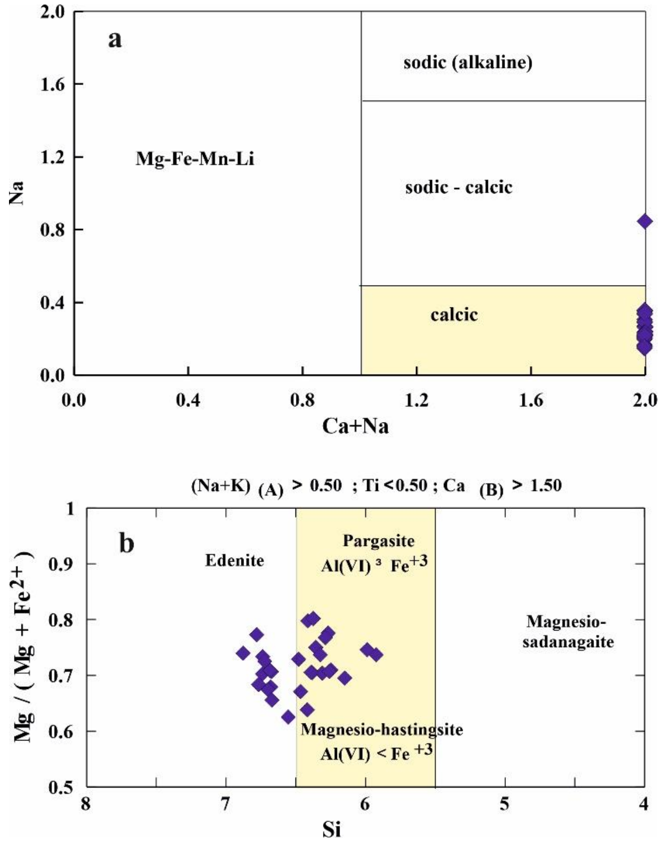

Figure 7. (a and b) The composition of amphiboles [51]. Symbols are as Fig. 5

Table 1. Minimum and maximum values of microprobe analyzes for plagioclase, hornblende, clinopyroxene, biotite and Fe-Ti oxide

	Plagioclase					**Hornblende**			
Rock types	Andesite (n=22)		Dacite (n=28)		**Rock types**	Andesite (n=13)		Dacite (n=18)	
	min	max	min	max		min	max	min	max
SiO_2	55.71	64.50	54.66	60.84	**SiO_2**	40.57	43.91	42.78	47.10
Al_2O_3	23.56	27.72	24.32	28.83	**TiO_2**	2.57	3.55	1.26	2.19
FeO	0.10	0.61	0.19	0.41	**Al_2O_3**	9.85	13.92	7.05	11.73

CaO	2.84	10.15	5.87	10.62	**FeO**	9.71	11.72	11.13	14.28
Na_2O	5.49	9.05	5.13	7.83	**MnO**	0.12	0.22	0.14	0.36
K_2O	0.07	1.66	0.29	0.74	**MgO**	14.42	15.16	13.30	14.99
Total	99.10	100.19	98.36	100.32	**CaO**	11.31	11.83	10.49	11.42
Si	10.05	11.30	9.88	10.86	**Na_2O**	2.24	2.82	1.39	2.27
Al	4.87	6.08	5.12	6.14	**K_2O**	0.84	1.27	0.45	0.84
Fe^{+2}	0.01	0.09	0.03	0.06	**Total**	96.85	98.51	96.44	97.45
Ca	0.53	1.96	1.12	2.06	**Si**	5.91	6.40	6.24	6.87
Na	1.93	3.08	1.80	2.72	**Ti**	0.28	0.39	0.14	0.24
K	0.02	0.38	0.07	0.17	**Al^{iv}**	1.59	6.15	1.12	1.75
An	14.69	48.45	28.56	52.43	**Al^{vi}**	0.00	0.32	0.09	0.38
Ab	48.78	84.85	45.88	67.27	**Fe^{+2}**	0.79	1.40	0.92	1.74
Or	0.45	9.78	1.69	4.17	**Fe^{+3}**	0.00	0.63	0.00	0.73
* structural formula on the basis of 23 oxygen atoms * n= sample number, min: minimum values, max: maximum values					**Mn**	0.01	0.03	0.02	0.05
					Mg	3.13	3.29	2.89	3.26
					Ca	1.77	1.85	1.64	1.79
					Na	1.27	1.59	0.57	1.28
					K	0.16	0.24	0.08	0.16
					Mg#	0.69	0.80	0.63	0.77

Table 1. continued

	Clinopyroxene			**Biotite**			**Fe-Ti oxide**			
Rock types	Andesite (n=14)		Rock types	Andesite (n=8)		Rock types	Andesite (n=7)		Dacite (n=6)	
	min	max		min	max		min	max	min	max
SiO_2	51.17	53.10	**SiO_2**	32.96	46.27	**SiO_2**	0.00	0.60	0.01	0.80
TiO_2	0.20	0.63	**TiO_2**	1.62	4.66	**TiO_2**	0.28	36.29	3.57	28.36
Al_2O_3	1.09	2.74	**Al_2O_3**	7.15	14.97	**Al_2O_3**	0.32	1.36	0.36	2.20
FeO*	7.00	8.95	**FeO**	13.07	15.47	**Cr_2O_3**	0.04	0.18	0.01	0.21
MnO	0.25	0.51	**MnO**	0.08	0.35	**FeO**	53.23	89.92	65.59	84.76
MgO	14.35	16.16	**MgO**	12.95	15.43	**MnO**	0.22	0.83	0.15	1.49
CaO	21.00	22.71	**CaO**	0.00	11.16	**MgO**	0.06	2.86	0.52	1.00
Na_2O	0.28	0.67	**Na_2O**	0.37	1.94	**CaO**	0.02	0.40	0.01	0.17
Total	99.35	101.26	**K_2O**	0.76	8.84	**Total**	90.01	93.17	93.03	96.58
Si	1.93	2.00	**Total**	91.33	98.07	**Si**	0.00	0.19	0.00	0.24
Ti	0.01	0.02	**Si**	2.62	3.30	**Ti**	0.07	8.52	0.82	6.48
Al	0.05	0.12	**Ti**	0.09	0.26	**Al**	0.12	0.50	0.13	0.79
Fe^{+3}	0.13	0.40	**Al**	0.60	1.32	**Cr**	0.01	0.05	0.00	0.05
Fe^{+2}	-0.18	0.15	**$Fe^{(ii)}$**	0.78	0.97	**$Fe^{(iii)}$**	0.00	15.68	2.86	13.03
Mn	0.01	0.02	**Mn**	0.01	0.02	**$Fe^{(ii)}$**	0.00	13.96	8.61	13.85
Mg	0.81	0.91	**Mg**	1.37	1.70	**Mn**	0.06	0.22	0.04	0.39
Ca	0.85	0.92	**Ca**	0.00	0.85	**Mg**	0.03	1.33	0.24	0.46
Na	0.02	0.05	**Na**	0.05	0.27	**Ca**	0.01	0.14	0.00	0.06
Wo	42.46	44.56	**K**	0.07	0.85	* structural formula on the basis of 32 oxygen atoms				
En	41.44	45.33	**Mg#**	0.62	0.66					
Fs	11.44	14.62								

Mg#	0.74	0.80	* structural formula on the basis of 22 oxygen atoms	
* 6 oxygen atoms				

4.2.3. Clinopyroxene

Clinopyroxenes mostly occur as euhedral and subhedral phenocrystals. Coarsely crystalline and euhedral clinopyroxenes in the rocks generally show zoning and occasionally a sieve texture. Structural formulas of clinopyroxenes were calculated according to 6 oxygen (Table 1). Clinopyroxenes in the andesite samples (Table 1) are classified as augite according to [52] (Figure 8). The composition of clinopyroxene, which is found as an inclusion, is augite. One of the samples shows zoning. The core of the zoning sample is diopside and the rim is augite (Table 1). The composition of augite is $Wo_{42-44}En_{41-45}Fs_{11-1}5$, while the Mg/Mg(Mg+$Fe^{+2}$) ratio is between 0.74 to 0.80. The inclusion augite has a composition of $Wo_{44}En_{42}Fs_{15}$, and its Mg/(Mg+Fe^{2+}) ratio is 0.74. The sample showing zoning has the composition of $Wo_{45}En_{44}Fs_{12}$ diopside in the core and the composition of $Wo_{44}En_{43}Fs_{13}$ augite at the rim, and the Mg/(Mg+Fe^{+2}) ratio is 0.80 in the core and 0.78 at the rim.

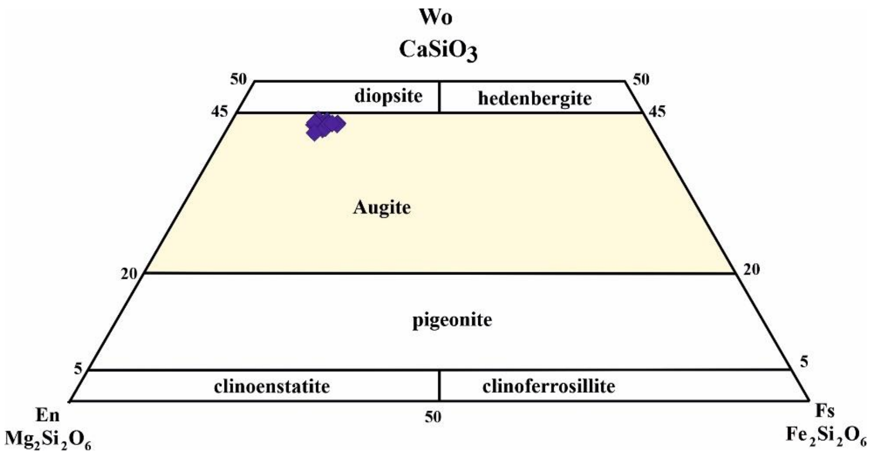

Figure 8. Classification diagram of pyroxene [52]

4.2.4. Biotite

Biotite occurs generally large and euhedral to subhedral. They are often found in association with clinopyroxene, Fe-Ti oxide minerals, and as inclusions within hornblende minerals (Figure 6). Their edges are partially resorbed, and they exhibit well-developed cleavage in one direction. Biotites are in phlogopite composition (Figure 9). Mg/(Mg+Fe^{+2}) values of phlogopites vary between 0.62 and 0.65 (Table 1).

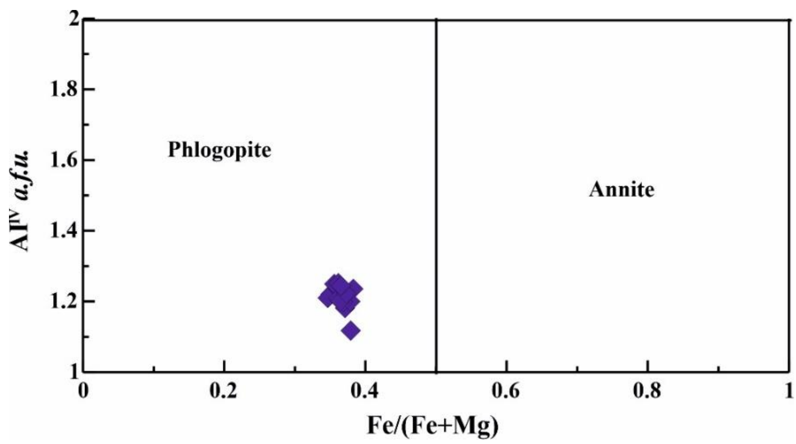

Figure 9. Biotite from the studied volcanic rocks on classification diagram [53]

4.2.5. Fe-Ti oxides

The Fe-Ti oxide in association with clinopyroxene and hornblende minerals, and their occasional occurrence as euhedral inclusions within these minerals, indicates relatively earlier crystallization. Fe-Ti oxides are generally found as inclusions in clinopyroxene and hornblende minerals, and in the composition of titano-magnetite and magnetite in the groundmass (Table 1, Figure 10).

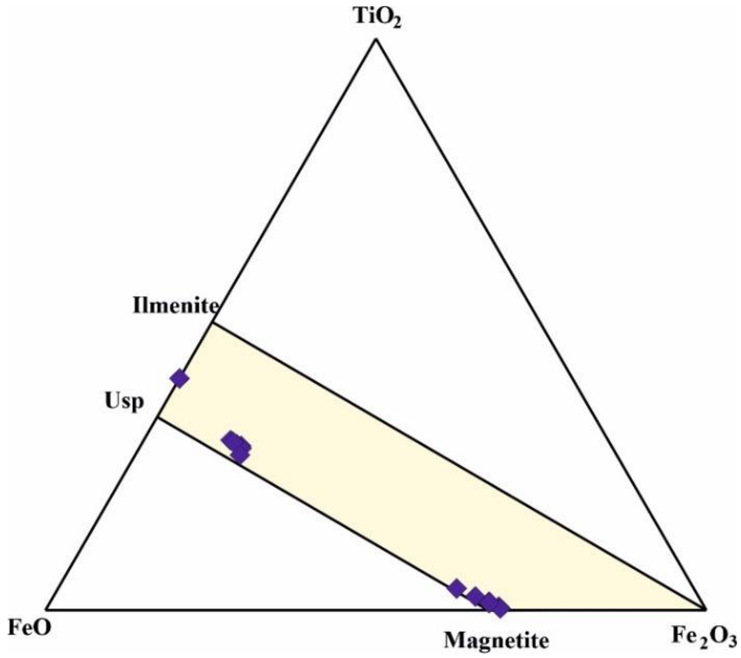

Figure 10. Classification ternary diagram [54]

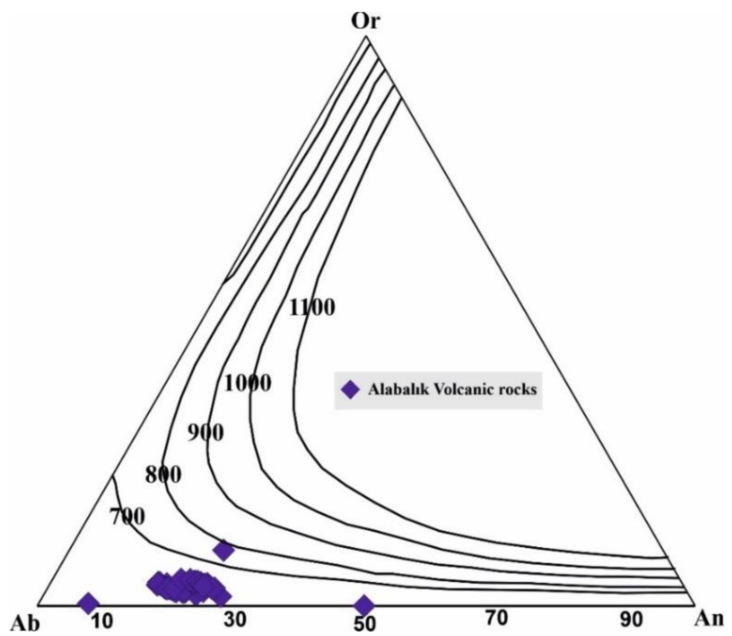

Figure 11. Determination of the crystallization temperatures of the plagioclases in the Alabalık Volcanics on the Ab-An-Or triangle diagram (temperature curves taken from [55]).

5. Discussion

5.1. Thermobarometric Calculations

5.1.1. Feldispar thermometer

The chemical compositions of the feldspars in the andesitic volcanic rocks are shown on the Ab-An-Or diagram for [55] geothermometer calculations (Figure 11). The Ab-An-Or contents of the plagioclase minerals are plotted on this diagram, the crystallization temperatures of the feldspars (plagioclase) in the Alabalık volcanic rocks generally vary from 600 to 800°C (Figure 11; Table 1).

5.1.2. Hornblende-plagioclase thermometer

According to the studies conducted by [56] using rocks from different geological areas, the temperatures calculated from rocks forming andesitic volcanic breccias range from 836 to 969 °C (average = 888 °C) (Table 3).

5.1.3. Amphibole thermobarometry, oxygen fugacity and hydrometer

[57] and [58] used microprobe analysis of amphiboles to estimate the P, T, H_2O content, ΔNNO, and fO_2 of the rocks. Additionally, pressures calculated according to [57] were between 1.3 and 8.4 kbar (mean = 3.2) (Table 2), with the temperatures of 820-1027 °C (mean = 902) (Table 3) for the Alabalık Volcanic rocks. According to [58], the estimated crystallization pressures are 1.3 ile 8.4 kbar (mean = 3.2), with the temperature values of 810-988 °C (mean = 904 °C), respectively (Table 2 and 3).

The pressure (P) of hornblende in the Alabalık volcanic rocks between 2.2 and 8.1 kbar (avg. = 4.7 kbar) according to [59], 2.1-8.8 kbar (mean = 5.0 kbar) according to [60], 1.7-6.7 kbar (mean = 3.8 kbar) according to [61] and 2.8-8.4 kbar (mean = 5.2 kbar) according to [62] (Table 2).

Another important factor in crystallisation processes in magmatic rocks is oxygen fugacity (fO_2) which is defined as partial pressure of oxygen. Oxygen fugacity controls the pressure-temperature correlations in melts and affects the stability intervals for rock-forming minerals. The oxygen fugacity values ($\log_{10} fO_2$) calculated with the approach proposed by [63], were between -15.2 to -12.6 for Alabalık volcanics (Table 4). The oxygen fugacity values calculated according to [57], using the Mg content of hornblendes in the volcanics are, respectively between -11.8 to -9.0 (Table 4). According to [57] and [58], the relative oxygen fugacity (ΔNNO) varies from 0.7-1.6 and 1.2-4.1, respectively.

The mean water (H_2O) content calculated according to [57] is 2.6 to 6.7 %, while mean water content was 4.1-8.2 % for volcanic rocks according to [58] (Table 4).

5.1.4. Biotite thermobarometry

The pressure and temperature values with biotite minerals [64] vary from 750-850 °C (mean. = 800 °C) and 0.7-1.5 kbar (mean = 1.5 kbar) [65] for the Alabalık Volcanic rocks (Table 2 and 3).

Table 2. The pressure estimates for the plutons calculated using hornblende-Al, hornblende and biotite barometers.

Alabalık Volcanics (n*)	**P1 (kbar) [60]**	**P2 (kbar) [61]**	**P3 (kbar) [62]**	**P4 (kbar) [63]**	**P5 (kbar) [57]**	**P6 (kbar) [57]**	**P7 (kbar) [57]**
	27	**27**	**27**	**27**	**27**	**27**	**14**
Min.	2.2	2.1	1.7	2.8	1.1	1.3	0.7
Max.	8.1	8.8	6.7	8.4	6.0	8.4	1.5
Avg.	4.7	5.0	3.8	5.2	2.5	3.2	1.3
Avg Deth (km)	17.6	18.3	14.1	19.2	9.1	12.0	5.0
* n: the number of analyses, depth was taken as 1kbar=3.7 km for the continental cru**st [66]**							

[a]Corresponding author: aydincakir61@gmail.com

Table 3. The temperature estimates calculated using hornblende-plagioclase.

Alabalık volcanics (n*)	**T ºC [56]**	**T ºC [57]**	**T ºC [58]**	**T ºC [64]**
	27	**27**	**27**	**14**
Min.	836	820	810	750
Max.	969	1027	988	850
Avg.	888	902	904	800
* n: the number of analyses				

Table 4. Oxygen fugacity and water content for plutons calculated using hornblende and biotite minerals.

Alabalık Volcanics (n*)	**[57]**			**[58]**		**[63]**
	ΔNNO	**fO_2**	**H_2O**	**ΔNNO**	**H_2O**	**fO_2**
	27	**27**	**27**	**27**	**27**	**14**
Min.	0.7	-11.8	2.6	1.2	4.1	-15.2
Max.	1.6	-9.0	6.7	4.1	8.2	-12.6
Mean	1.1	-10.8	4.8	2.2	5.7	-13.9
* n: the number of analyses						

5.1.5. Clinopyroxene thermobarometry

[67] and [68] proposed a pyroxene geothermometer in which isotherm curves representing various temperature values were on the Di-Hd-En-Fs pyroxene quadrilateral, creating a thermometer diagram (Figure 12). The compositions of pyroxenes plotted on this diagram must satisfy the condition Wo+En+Fs ≥90. When the compositions of the clinopyroxene minerals are plotted on this diagram, the crystallization temperatures of clinopyroxenes generally range between 600-800°C in volcanic rock samples (Figure 12).

[69] performed experimental observations and calculated the Fe-Mg exchange constant KD(Fe–Mg) for clinopyroxene-melt equilibrium to be 0.27 ± 0.03. The calculated results of the studied rocks show temperatures ranging from 1129 to 1183 ºC and pressures ranging from 4.9 to 8.6 kbar (Table 5).

The corresponding crystallization depth for the obtained average clinopyroxene pressure values is 18-29 km (for continental crust, 1 kbar = 3.7 km, [66]. This indicates that the volcanic rocks are situated within the shallow to mid-crustal magma chambers.

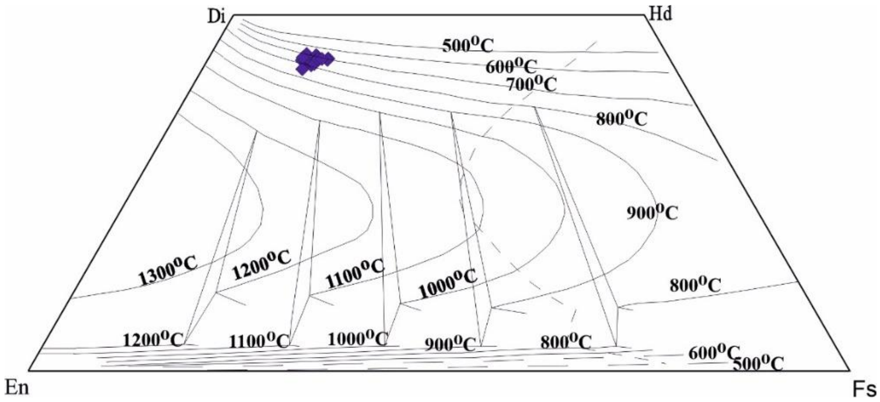

Figure 12. Di-Hd-En-Fs pyroxene quadrilateral showing the compositions of clinopyroxenes in the Alabalık Volcanics. Isotherm curves are constructed at intervals of 100°C and under 1 atm pressure [67, 68]

Table 5. Clinopyroxene temperature and pressure calculations

	[69]	
	T (32d, ºC)	**P (32c, kbar)**
Alabalık Volcanics (n*)	**6**	**6**
Min.	1129	4.9
Max.	1183	8.6
Avg.	1162	7.3
Avg. Dept. (km)		25.9
* n: the number of analyses, depth was taken as 1kbar=3.7 km for the continental crust [66]		

6. Conclusion

- Petrographically, the studied volcanic rocks comprise of mainly plagioclase, hornblende, biotite, clinopyroxene and Fe-Ti oxide minerals.
- They have some textural features indicating disequilibrium crystallization such as; sieve and oscillatory zoned plagioclase, the presence of normally and reversely zoned plagioclase in the same sample, the poikilitic textures.
- According to thermobarometer estimations, the investigated volcanic rocks have pressures from 4.9 to 6.8 kbar, temperature from 1129 to 1183 °C, oxygen fugacity values from -15.2 to -9.0 and water contents of 2.6-8.2 %.
- Considering field, petrographic and thermobarometric data, the magmas that forms the studied volcanic rocks had undergone hydrous crystallizations in the shallow to mid-crustal magma chambers.

7.Acknowledgement

This work was financially supported by the Scientific Research Projects Foundation of Gümüşhane University (Project number: 22.F5114.01.02). An anonymous reviewer is thanked for their general improvement of the manuscript.

8.References

[1] Şengör AMC, Yılmaz Y. Tethyan Evolution of Turkey: A Plate Tectonic Approach. Tectonophysics 1981; 75:181241.

[2] Okay AI, Şahintürk O. Geology of The Eastern Pontides, In: A. G. Robinson, (Ed.), Regional and Petroleum Geology of The Black Sea and Surrounding Region. AAPGMem 1997; 68:291-311.

[3] Yılmaz Y, Tuysuz O, Yigitbas E, Genc SC, Sengor AMC. Geology and tectonic evolution of the Pontides, in Robinson, A.G. ed. Regional and petroleum geology of the black sea and surrounding region, Volume 68: Tulsa, Oklahoma: The American Association of Petroleum Geologists 1997; 183–226.

[4] Keskin M, Genç ŞC, Tüysüz O. Petrology and Geochemistry of Postcollisional Middle Eocene Volcanic Units In North-Central Turkey: Evidence for Magma Generation By Slab Breakoff Following The Closure of The Northern Neotethys Ocean. Lithos 2008; 104:267–305.

[5] Kaygusuz A, Aslan Z, Siebel W, Şen C. Geochemical and Sr-Nd isotopic characteristics of post-collisional calc-alkaline volcanics in the Eastern Pontides (NE Turkey), Turk J Earth Sci 2011; 20:137–159.

[6] Arslan M, Temizel İ, Abdioğlu E, Kolaylı H, Yücel C, Boztuğ D, Şen C. ^{40}Ar-^{39}Ar Dating, Whole-Rock and Sr-Nd-Pb Isotope Geochemistry of Post-Collisional Eocene Volcanic Rocks In The Southern Part of The Eastern Pontides (NE Turkey): İmplications for Magma Evolution In Extension-İnduced Origin. Contributions to Mineralogy and Petrology 2013; 166:113-142.

[7] Aydınçakır E, Şen C. Petrogenesis of the postcollisional volcanic rocks from the Borçka (Artvin) area: implications for the evolution of the Eocene magmatism in the Eastern Pontides (NE Turkey). Lithos 2013; 172-173: 98–117.

[8] Yücel C, Arslan M, Temizel İ, Abdioğlu Y. Ruffet G. Evolution of K-rich Magmas Derived From A Net Veined Lithospheric Mantle İn An Ongoing Extensional Setting: Geochronology and Geochemistry of Eocene and Miocene Volcanic Rocks From Eastern Pontides (Turkey). Gondwana Research 2017; 45:65–86.

[9] Dokuz A, Aydin F, Karsli O. Postcollisional transition from subduction-to intraplate-type magmatism in the eastern Sakarya zone, Turkey: Indicators of northern Neotethyan slab breakoff, Geol. Soc. Am. Bull. 2019; 131:1623–1642.

[10] Aydınçakır E, Yücel C, Ruffet G, Gücer MA, Akaryalı E, Kaygusuz A. Petrogenesis of Post-collisional Middle Eocene Volcanism in the Eastern Pontides (NE, Turkey): Insights from Geochemistry, Whole-rock Sr-Nd-Pb isotopes, Zircon U-Pb and ^{40}Ar-^{39}Ar geochronology. Geochemistry 2022; 82:125871.
[11] Kaygusuz A, Yücel C, Aydınçakır E, Gücer MA, Ruffet G. Petrogenesis of the Middle Eocene calc-alkaline volcanic rocks in the Bayburt area Eastern Pontides (NE Turkey): Implications for Magma evolution in extension-related Setting. Mineralogy and Petrology 2022; 116:379–399.
[12] Topuz G, Okay AI, Altherr R, Schwarz WH, Siebel W, Zack T, Satir M, Şen C. Post-collisional adakite-like magmatism in the Ağvanis massif and implications for the evolution of the Eocene magmatism in the Eastern Pontides (NE Turkey). Lithos 2011; 125:131–150.
[13] Karsli O, Uysal İ, Ketenci M, Dokuz A, Aydin F, Kandemir R, Wijbrans J. Adakite-like granitoid porphyries in Eastern Pontides, NE Turkey: Potential parental melts and geodynamic implications. Lithos 2011; 127:354–372.
[14] Dokuz A, Uysal İ, Meisel W, Turan M, Duncan R, Akçay M. Post-collisional adakitic volcanism in the eastern part of the Sakarya Zone, Turkey: evidence for slab and crustal melting. Contributions to Mineralogy and Petrology 2013; 166:1443–1468.
[15] Aydın F. 2014. Geochronology, geochemistry, and petrogenesis of the Maçka subvolcanic intrusions: implications for the late Cretaceous magmatic and geodynamic evolution of the eastern part of the Sakarya zone, northeastern Turkey. International Geology Review 2014; 56:1246-1275.
[16] Boztuğ D, Jonckheere RC, Wagner GA, Yeğingil Z. Slow Senonian and fast Palaeocene–Early Eocene uplift of the granitoids in the central eastern Pontides, Turkey: Apatite fission-track results: Tectonophysics 2004; 382(3–4):213–228.
[17] Şengör AMC, Özeren S, Genç T, Zor E. East Anatolian High Plateau As A Mantlesupported, North–south Shortened Domal Structure. Geophysical Research Letters 2003; 30(24):8045.
[18] Topuz G, Altherr R, Kalt A, Satir M, Werner O, Schwarz WH. Aluminous granulites from the Pulur complex NE Turkey: a Case of Partial Melting, Efficient Melt Extraction and Crystallization. Lithos 2004; 72:183–207.
[19] Topuz G, Altherr R, Schwarz WH, Dokuz A, Meyer HP. Variscan amphibolite-facies rocks from the Kurtoğlu metamorphic complex (Gümüşhane area, Eastern Pontides, Turkey): International Journal of Earth Sciences 2007; 96(5):861–873.
[20] Okay AI, Satır M, Siebel W. Pre-Alpide Palaeozoic and Mesozoic orogenic events in the Eastern Mediterranean region. In: Gee, D.G., Stephenson, R.A. (Eds.), European Lithosphere Dynamics. Geological Society, London, Memoirs 2006; 32:389–405.
[21] Dokuz A, Uysal İ, Kaliwoda M, Karslı O, Ottley CJ, Kandemir R. Early abyssal- and late SSZ-type vestiges of the Rheic oceanic mantle in the Variscan basement of the Sakarya Zone, NE Turkey: implications for the sense of subduction and opening of the Paleotethys. Lithos 2011; 127:176–191.
[22] Çoğulu E. Gümüşhane ve Rize granitik plutonlarının mukayeseli petrojeolojik ve jeokronolojik etüdü. Unpubl Diss Thesis, İstanbul Tech Univ 1975.
[23] Topuz G, Altherr R, Siebel W, Schwarz WH, Zack T, Hasözbek A, Barth M, Satır M, Şen C. Carboniferous high-potassium I-type granitoid magmatism in the Eastern Pontides: the Gümüşhane Pluton (NE Turkey). Lithos 2010; 116:92–110.
[24] Kaygusuz A, Arslan M, Wolfgang S, Sipahi F, İlbeyli N. Geochronological evidence and tectonic signifi cance of Carboniferous magmatism in the southwest Trabzon area, eastern Pontides, Turkey. International Geology Review 2012; 54(15):1776–1800.
[25] Kaygusuz A, Arslan M, Sipahi F, Temizel İ. U-Pb zircon chronology and petrogenesis of Carboniferous plutons in the northern part of the Eastern Pontides, NE Turkey: constraints for Paleozoic magmatism and geodynamic evolution. Gondwana Research 2016; 39:327–346.
[26] Karslı O, Dokuz A, Kandemir R. Subduction-related Late Carboniferous to Early Permian Magmatism in the Eastern Pontides, the Camlik and Casurluk plutons: Insights from geochemistry, whole-rock Sr–Nd and in situ zircon Lu–Hf isotopes, and U–Pb geochronology. Lithos 2016; 266–267:98–114.
[27] Dokuz A, Külekçi E, Aydınçakır E, Kandemir R, Alçiçek MC, Pecha ME, Sünnetçi K. Cordierite-bearing strongly peraluminous Cebre Rhyolite from the eastern Sakarya Zone, NE Turkey: Constraints on the Variscan Orogeny. Lithos 2017a; 278–281:285–302.
[28] Okay Aİ, Leven EJ. Stratigraphy and paleontology of the upper Paleozoic sequences in the Pulur (Bayburt) region, Eastern Pontides. Turkish Journal of Earth Sciences 1996; 5:145-155.

[29] Kandemir R, Lerosey-Aubril R. First report of a trilobite in the Carboniferous of Eastern Pontides, NE Turkey. Turkish Journal of Earth Sciences 2011; 20:179–183.
[30] Saydam Eker Ç, Sipahi F, Kaygusuz A. Trace and rare earth elements as indicators of provenance and depositional environments of Lias cherts in Gumushane, NE Turkey. Chemie der Erde Geochemistry 2012; 72:167–177.
[31] Dokuz A, Aydincakir E, Kandemir R, Karslı O, Siebel W, Derman AS, Turan M. Late Jurassic magmatism and stratigraphy in the eastern Sakarya Zone, Turkey: evidence for the slab breakoff of Paleotethyan oceanic lithosphere. Journal of Geology 2017b; 125: 1–31.
[32] Eyüboğlu Y, Dudas FO, Santosh M, Xiao Y, Yi K, Chatterjee N, Wu FY, Bektaş O. Where are the remnants of a Jurassic Ocean in the Eastern Mediterranean Region? Gondwana Research 2016; 33:63–92.
[33] Karslı O, Dokuz A, Kandemir R. Zircon Lu-Hf isotope systematics and U-Pb geochronology, whole-rock Sr-Nd isotopes and geochemistry of the early Jurassic Gökçedere pluton, Sakarya Zone-NE Turkey: a magmatic response to roll-back of the Paleo-Tethyan oceanic lithosphere. Contributions to Mineralogy and Petrology 2017; 172: 1–31.
[34] Aydınçakır E, Yücel C, Kaygusuz A, Bilici Ö, Yi K, Jeong YJ, Güloğlu ZS. Magmatic evolution of the Calc-alkaline Middle Jurassic igneous rocks in the eastern pontides, NE Turkey: insights from geochemistry, whole-rock Sr-Nd-Pb, in situ zircon Lu-Hf isotopes, and U-Pb geochronology, International Geology Review 2023; 65(20): 3146-3167.
[35] Aydınçakır E. The Petrogenesis of Early-Eocene non-adakitic volcanism in NE Turkey: constraints on geodynamic implications. Lithos, 2014; 208: 361–377.
[36] Eyuboglu Y, Santosh M, Chung SL. Petrochemistry and U-Pb Zircon Ages of Adakitic Intrusions from the Pulur Massif (Eastern Pontides, NE Turkey): Implications for Slab Rollback and Ridge Subduction Associated with Cenozoic Convergent Tectonics in the Eastern Mediterranean. The Journal of Geology 2011; 119: 394–417.
[37] Karsli O, Chen B, Aydin F, Şen C. Geochemical and Sr–Nd–Pb isotopic compositions of the Eocene Dölek and Sariçiçek Plutons, Eastern Turkey: implications for magma interaction in the genesis of high-K calc-alkaline granitoids in a post-collision extensional setting. Lithos 2007; 98:67–96.
[38] Karslı O, Dokuz A, Uysal İ, Ketenci M, Chen B, Kandemir R. Deciphering the shoshonitic monzonites with I-type characteristic, the Sisdağı pluton, NE Turkey: magmatic response to continental lithospheric thinning. Journal of Asian Earth Sciences 2012; 51:45-62.
[39] Aydın F, Karslı O, Chen B. Petrogenesis of the Neogene alkaline volcanics with implications for post collisional lithospheric thinning of the Eastern Pontides, NE Turkey. Lithos; 2008; 104:249–266.
[40] Kaygusuz A, Aslan Z, Aydınçakır E, Yücel C, Gücer MA, Şen C. Geochemical and Sr-Nd-Pb isotope characteristics of the Miocene to Pliocene volcanic rocks from the Kandilli (Erzurum) area, Eastern Anatolia (Turkey): Implications for magma evolution in extension-related origin. Lithos 2018; 296/299:332-351.
[41] Temizel I, Arslan M, Yücel C, Abdioğlu-Yazar E, Kaygusuz A, Aslan Z. Eocene tonalite-granodiorite from the Havza (Samsun) area, northern Turkey: Adakite-like melts of lithospheric mantle and crust generated in a post-collisional setting: International Geology Review 2020; 62:1131–1158.
[42] Kaygusuz A. K/Ar ages and geochemistry of the collision related volcanic rocks in the Ilıca (Erzurum) area, eastern Turkey. N. Jahrb. Mineral 2009; 186 (1):21–36.
[43] Karslı O, Chen B, Uysal I, Aydın F, Wijbrans JR, Kandemir R. Elemental and Sr- Nd-Pb Isotopic Geochemistry of The Most Recent Quaternary Volcanism In The Erzincan Basin, Eastern Turkey: Framework For The Evalution of Basalt-Lower Crustinteraction. Lithos 2008; 106:55–70.
[44] Karsli O, Caran Ş, Çoban H, Şengün F, Tekkanat O, Andersen T. Melting of the juvenile lower crust in a far-field response to roll-back of the southern Neotethyan oceanic lithosphere: The Oligocene adakitic dacites, NE Turkey: Lithos 2020; 370–371:105614.
[45] Eyuboglu Y, Santosh M, Yi K, Bektaş O, Kwon S. Discovery of Miocene adakitic dacite from the Eastern Pontides Belt and revised geodynamic model for the late Cenozoic Evolution of eastern Mediterranean region. Lithos 2012; 146–147: 218–232.
[46] Yücel C. Geochronology, geochemistry, and petrology of adakitic Pliocene–Quaternary volcanism in the Şebinkarahisar (Giresun) area, NE Turkey. International Geology Review 2019; 61(6):754-777.
[47] Okay AI, Tüysüz O. Tethyan sutures of northern Turkey. Geol. Soc. Lond. Spec. Publ 1999; 156: 475–515.

[48] Güven İH. 1/250 000 scaled geological and metallogenical map of the Eastern Black Sea Region. – General Directorate of Mineral Research and Exploration, Ankara1993.
[49] Konak N, Hakyemez HY. Tectonic Units of The Easternmost Part of The Pontides: Stratigraphical and Structural Implications, Proceedings of The 2nd Int. Symp. On the Petroleum Geology and Hydrocarbon Potential of The Black Sea Area. Turkish Association of Petroleum Geologists, Spec. Publ 2001; 4:93-103.
[50] Shelley D. Igneous and metamorphic rocks under the microscobe, Chapman and Hall, London 1993:445 pp.
[51] Leake EB, Wooley AR, Arps CES, Birch WD, Gilbert MC, Grice JD, Hawthorne FC, Kato A, Kisch HJ, Krivovichev VG, Linthout K, Laird J, Mandarino J, Maresch WV, Nickhel EH, Rock NMS, Schumacher JC., Smith DC, Stephenson NCN, Ungaretti L, Whittaker EJW, Youzhi G. Nomenclature of amphiboles report of the subcommittee on amphiboles of the International Mineralogical Association Commission on New Minerals and Mineral Names, European Journal of Mineralogy 1997; 9:623-651.
[52] Morimoto M, Fabries J, Ferguson AK, Ginzburg IV, Ross M, Seifert FA, Zussman J, Aoki K, Gottardi G. Nomenclature of Pyroxenes. Mineralogical Magazine 1988; 52:535-550.
[53] Speer JA. Micas in igneous rocks. In S. W. Bailey (Ed.), Micas: Reviews in mineralogy and geochemistry, Washington, DC. Mineralogical Society of America 1984; 13:299–356.
[54] Bacon CR, Hirschmann MM. Mg/Mn Partirioning As A Test for Equilibrium Between Coexisting Fe-Ti Oxides. American Mineralogist, 1988; 13:57-61.
[55] Fuhrman ML, Lidsley DH. Ternary-feldspar Modelling and Thermometry, American Mineralogist 1988; 73:201-215.
[56] Holland TJB, Blundy JD. Non-ideal interactions in calcic amphiboles and their bearing on amphibole-plagioclase thermometry. Contribution to Mineralogy and Petrology 1994; 116:433-447.
[57] Ridolfi F, Renzulli A, Puerini M. Stability and chemical equilibrium of amphibole in calc-alkaline magmas: an overview, new thermobarometric formulations and application to subduction- related volcanoes. Contributions to Mineralogy and Petrology 2010; 160:45–66.
[58] Ridolfi F, Renzulli A. Calcic amphiboles in calcalkaline and alkaline magmas: thermobarometric and chemometric empirical equations valid up to 1,130°C and 2.2 Gpa. Contributions to Mineralogy and Petrology 2012; 163:877–895.
[59] Hammarstrom JM, Zen E. Aluminum in amfi bole: An empirical igneous geobarometer. American Mineralogist 1986; 71:1297–1313.
[60] Johnson MC, Rutherford MJ. Experimental calibration of the aluminiun-in amfibole geobarometer with application to Long Valley Caldera (California) volcanic rocks. Geology 1989; 17:837–841.
[61] Hollister LS, Grisson GC, Peters EK, Stowell HH, Sisson VB. Confi rmation of the empirical calibration of aluminum in amfibole with pressure of solidifi cation of calc-alkaline plutons. American Mineralogist 1987; 72:231–239.
[62] Schmidt MW. Amphibole composition in tonalite as a function of pressure: An experimental calibration of the Al-in amfibole barometer. Contributions to Mineralogy and Petrology 1992; 110:304–310.
[63] Wones DR. Signifi cance of the assemblage titanite + magnetite + quartz in granitic rocks. American Mineralogist 1989; 74:744–749.
[64] Luhr JF, Carmichael ISE, Varekamp JC. The 1982 eruptions of El Chicón Volcano, Chiapas, Mexico: Mineralogy and petrology of the anhydrite bearing pumices. Journal of Volcanology and Geothermal Research 1984; 23:69–108.
[65] Uchida E, Endo S, Makino M.. Relationship between solidification depth of granitic rocks and formation of hydrothermal ore deposits. Resource Geology 2007; 57:47–56.
[66] Tulloch AJ, Challis GA.. Emplacement depths of Paleozoic–Mesozoic plutons from western New Zealand estimated by hornblende-Al geobarometry. New Zealand Journal of Geology and Geophysics 2000; 43:555-567.
[67] Lindsley DH. Pyroxene Thermometry. American Mineralogist, 1983; 68:477-493.
[68] Lindsley DH, Andersen DJ. A Two-Pyroxene Thermometer. Journal of Geophysical Research 1983; 88:A887-A906.
[69] Putirka KD. Thermometers and Barometers for Volcanic Systems. In Putirka KD, Tepley FE, Reviews in Mineralogy and Geochemistry 2008; 69:61120.